Design of electrically driven single photon source based on dielectric passive cavity structure at 1.3 μm

S A Blokhin[1], M A Bobrov[1], N A Maleev[1], A A Blokhin[2], A P Vasyl'ev[2], A G Kuzmenkov[2],V A Shchukin[3,4], N N Ledentsov[4], S Reitzenstein[3] and V M Ustinov[2]

[1] Ioffe Institute, St. Petersburg, 194021 Russia
[2] Research and Engineering Center for Submicron Heterostructures for Microelectronics, St. Petersburg, 194021 Russia
[3] Technische Universität Berlin, Berlin, D-10623 Germany
[4] VI Systems GmbH, Berlin, D-10623 Germany
E-mail: blokh@mail.ioffe.ru

Abstract. A combination of advanced concepts is applied for designing micro-cavity structures aimed for single-photon sources with high photon-extraction efficiency in the telecom O-band at ~1.3 μm. The device design consists of a broad stop-band bottom distributed Bragg reflector (DBR), a top DBR formed in a dielectric micropillar with additional circular Bragg grating and a central dielectric passive cavity. This combination of photonic elements is compatible with electric carrier injection and provides overall photon-extraction efficiency of ~83% as shown by 3D finite-difference time-domain simulations.

The development of quantum-light sources based on semiconductor quantum dots (QDs) has become a central research area in nanophotonics. The emitted single photons can be used as information carriers in long-distance quantum communication and/or photonic qubits in quantum circuits [1]. The design of single-photon source (SPS) must provide not only a narrow far field to foster the in-coupling to optical fibers in future applications, but also a high photon-extraction efficiency. The extraction efficiency of a QD in a simple planar semiconductor is fairly small (<2%), but the fabrication of monolithic micro-lenses upon pre-selected QDs in combination with a bottom distributed Bragg reflector (DBR) can lead to broadband enhancement of the photon-extraction efficiency to ~29% under optical excitation [2]. Another approach using photonic wires or photonic trumpets allows one to increase the extraction efficiency of QD emission to ~72% under optical excitation, but the fabrication of the electrically driven SPSs is quite challenging in this case [3]. Embedding single QDs into narrow-band micopillar cavities makes it possible to achieve photon-extraction efficiency up to ~74% under optical excitation [4], and up to ~61% under electrical excitation [5]. More recently, photon-extraction efficiencies up to 85% have been reported for single-photon sources based on circular Bragg gratings, which, however, are not compatible with electrical carrier injection [6]. It should be noted that most of the works on efficient QD single-photon sources have focused on the short wavelength range (GaAs QD emitting at 780 nm or InGaAs QDs emitting at ~900-960 nm), while quantum-light sources at telecom O-band wavelengths still suffer from low photon-extraction efficiency. In fact, a photon extraction efficiency of 3.3% was reported for micropillar cavity based on InAs/GaAs bilayer QDs [7], 10% (within a numerical aperture of 0.4) for a deterministically fabricated microlense structures based on InGaAs/GaAs bilayer QDs [8] and 36% (within a numerical aperture of 0.7) for a photonic crystal cavity based on InAs/InP QDs [9].

Therefore, the development of bright 1.3 μm SPSs with narrow far-field suitable for single-mode fiber coupling and electrical excitation is an important task to advance the application of such quantum devices for instance in fiber-based quantum communication. Interestingly, in a recent work the circular Bragg grating concept has been extended to the telecom wavelength range in a numeric study which promises photon-extraction efficiencies up to 95% in optical pumped devices [10]. In this work, we describe numeric modeling and optimization of different designs for electrically driven SPSs emitting at 1.3 μm. Exploiting the passive cavity concept and circular Bragg grating we proposed a cavity design for photon-extraction efficiency of ~83%.

The 3-D finite-difference time-domain (FDTD) method is used for the detailed investigation of the different types of microcavity geometries and to evaluate the influence of different design elements on the photon-extraction efficiency of the light-emitting structures under investigation. For each type of microcavity a subwavelength grid model was build. The grid size in the vertical direction is 20 nm, while in the lateral direction it is 30 nm which suffices for smooth in–plane variations of the optical field. To simplify the calculations free-carrier absorption in doped layers was neglected. The QD itself can be approximated by a dipole source with in-plane dipole moment. The light emitter with linear polarization along the X-direction is placed at the center of the active cavity to excite the fundamental mode HE_{11} (see Fig. 1a). The FDTD method calculates the microcavity response at its resonance frequency in the time domain triggered by a short excitation pulse applied to the dipole. Using the broadband dipole source ehe actual mode spectrum of microcavity can be obtained by the Fourier transform of the microcavity response. The analysis of the lateral distribution (X-Y plane) of the electromagnetic field inside the cavity at the microcavity's resonance frequencies allows one to identify the mode type in each case and select the resonance frequency corresponding to the fundamental mode HE_{11}. To estimate the part of light emitted from the top and bottom of the cavity and lateral optical losses we calculate the energy flux passing through the corresponding planes of a probe box surrounding the microcavity (indicated by the green dashed line in Fig. 1a) and compare this to the total energy flux passing through a probe box surrounding the dipole source. Since in the present approach the coupling efficiency of the extracted light to the fundamental mode of the single-mode fiber depends on the degree of overlap between the near-field emission pattern of the investigated microcavity at the respective distance and the Gaussian mode of the used single-mode fiber, the high coupling efficiency to the single-mode fiber can be achieved in the near-filed coupling regime [10-11]. Hence, we have analyzed the near-field emission pattern at the fixed distance (3 μm) from the top surface of the investigated microcavity. The overall photon-extraction efficiency within a numerical aperture (NA) of 0.7 was calculated based on the near-field emission pattern. Note that the calculated efficiency becomes independent of the lateral grid size once the latter is smaller than 40 nm.

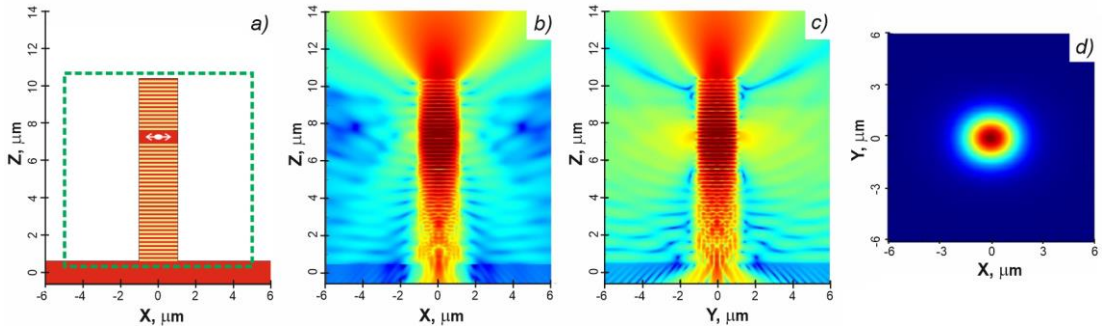

Figure 1. 1.3 μm range circular micro-pillar based on 2λ-cavity semiconductor structure: refractive index profile in X-Z plane (a) and on-resonance electric field intensity distribution in X-Z (b), Y-Z (c), X-Y (d) planes for the fundamental mode HE_{11}.

First we consider the reference case of an electrically driven SPS based on a single QD embedded in a circular semiconductor micro-pillar microcavity with top and bottom distributed Bragg reflectors (DBRs). For creating electrically driven SPS, the micro-pillar diameter of ~2 μm was chosen to reliably achieve maximum photon-extraction efficiency by an optimized balance between Purcell-enhanced

light-matter interaction and low lateral photon losses as discussed in more detail for instance in [5]. Figure 1 shows cross-section images representing the results of the simulation of this case. The microcavity consists of a 2λ-thick GaAs-cavity surrounded by p-type top and n-type bottom GaAs/AlAs DBRs (see Figure 1.a). The top and bottom DBRs have 13 and 30 mirror pairs, respectively. Strong confinement of the electromagnetic field of the fundamental mode inside the circular micro-pillar is clearly seen. The difference in the reflectivity of the top and bottom DBRs provides the light extraction from the top plane of the probe box up to 84% with the sidewall leakage of about 7%. Light scattering at the pedestal of the circular micro-pillar leads to the mode coupling between the fundamental and higher order modes [12], which increases the unwanted bottom leakage up to 9%. Hence the overall photon-extraction efficiency reaches 78% within NA of 0.7. Such high extraction efficiency is comparable with state-of-the-art values of 74% and 61% obtained in the 930 nm range QD-based 1λ-thick micropillars under optical and electrical excitation, respectively [4-5]. Note that an additional ring trench pattern created the 2nd-order radial Bragg grating can provide the strong suppression of side emission in the microcavity pillar (not shown), but it comes at the price of enhanced bottom leakage up to 12% and, therefore, the overall extraction efficiency (NA=0.7) will increase only by 4%. However the high emission divergence limits the efficiency of optical coupling to a standard single-mode fiber, typically, at about 4%.

The development of the bright electrically driven SPSs emitting in the 1.3μm wavelength range is a stronger challenge as compared to the short-wavelength range counterparts due to huge free-carrier absorption in p-type doped layers [13]. The most straightforward approach is to use a microcavity design with carrier injection through intra-cavity contact layers (IC layers) to minimize the mentioned absorption losses. We analyze a microcavity consisting of a 2λ-thick central GaAs-cavity with n-type and p-type IC-layers surrounded by undoped top and bottom GaAs/AlAs DBRs (see Figure 2.a). The reflectivity of the top and bottom DBRs are the same to those in the previous structure with doped DBRs. Figure 2 shows cross-section images representing the simulation results of the semiconductor microcavity structure with IC-layers, where the micro-pillar can be formed only in top DBR (hereinafter referred to as half-pillar) as the current path cannot be provided otherwise. The side emission is apparently strongly enhanced with some evidence of a complex mode structure due to the weaker lateral mode confinement. In fact, the sidewall leakage rises up to 53%, while the part of emission from the bottom of the cavity remains around 9%. As a result the overall extraction efficiency (NA=0.7) drastically falls down to 34% in this electrically operational SPS.

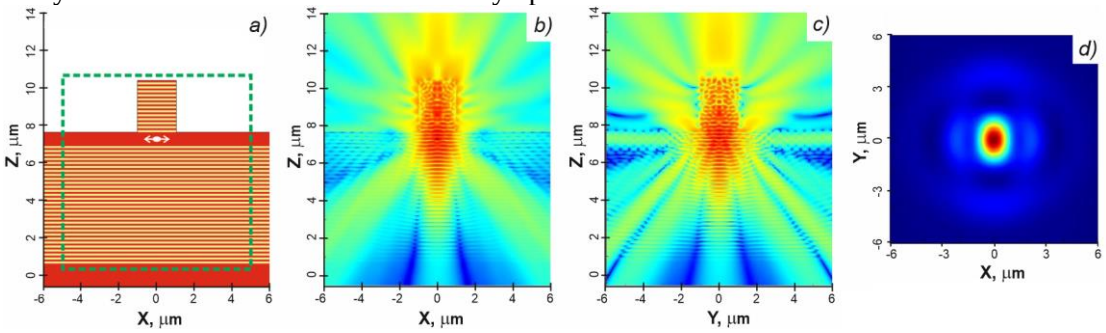

Figure 2. 1.3 μm range circular half-pillar based on a 2λ-cavity semiconductor structure with IC-layers: refractive index profile in X-Z plane (a) and on-resonance electric field intensity distribution in X-Z (b), Y-Z (c), X-Y (d) planes for the fundamental mode HE_{11}.

To reduce the carrier injection area into the QD-based active region and improve the carrier injection efficiency into the single QD, an oxide current aperture with a 2 μm-diameter was inserted in the cavity. Noteworthy, the 40 nm-thick oxide-confined aperture placed at one of the local intensity maxima of the vertical mode field (antinode) can slightly redistribute the optical field inside the cavity and decrease the sidewall leakage only by 5% (not shown). As a result it leads only to a moderate increase of the photon-extraction efficiency to a value of 35% (NA=0.7).

To improve the photon-extraction efficiency of SPS with IC design we consider an extended design with a radial Bragg grating surrounding the upper half-pillar. As shown in Figure 3, the use of the radial 2nd-order trench pattern etched through the top DBR around the central region can partially suppress the sidewall leakage via the top DBR, however it cannot block the light propagation out of the cavity below the top DBR. Moreover, the insertion of the radial Bragg grating enhanced the bottom leakage up to 16% and, as a result, the extraction efficiency is nearly unchanged. The significant transformation of the near-field pattern, possibly, due to the mode coupling between the fundamental and higher order modes will degrade the coupling efficiency of the emission into standard single-mode fiber with NA~0.12.

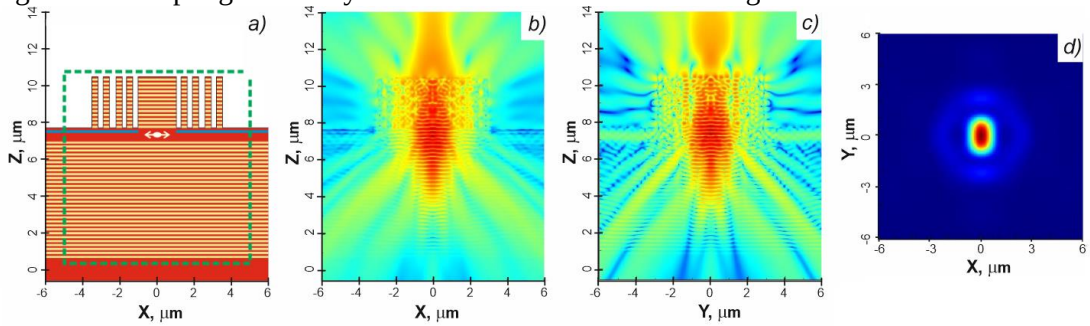

Figure 3. 1.3 μm range circular radial DBR microcavity half-pillar based on a 2λ-cavity semiconductor structure with IC layers and oxide-confined aperture: refractive index profile in X-Z plane (a) and on-resonance electric field intensity distribution in X-Z (b), Y-Z (c), X-Y (d) planes for the fundamental mode HE_{11}.

In order to suppress the light propagation in the direction towards the substrate at tilted angles, to redirect upward the emission from cavity and to reduce the emission passing through the sides of the top DBR both DBRs should have a broad stop-band. The wet selective oxidation of AlGaAs layers provides a huge refractive index step of about 1.9-2 between GaAs and $AlGa_xO_y$ layers, hence the selectively oxidized GaAs/$AlGa_xO_y$ DBR allows for efficient light reflection in a broad range light incidence. Note that the dielectric DBR based on SiO_2/Ta_2O_5 layers also can help to decrease lateral losses by increasing the angle range for light reflection due to a 2-fold broader stop-band with a width of ~260 nm as compared to the GaAs/AlAs DBRs. The microcavity consists of a 2λ-thick GaAs-cavity with n-type and p-type IC-layers and a thin oxide-confined aperture surrounded by bottom GaAs/$AlGa_xO_y$ DBR and top SiO_2/Ta_2O_5 DBR (see Figure 4.a). The parameters of the top and bottom DBRs for a hybrid 2λ-cavity structure are designed such that the mirrors have reflectivity similar to the previous structures. Figure 4 shows cross section images representing the results of the simulation of the circular half-pillar based on the hybrid 2λ-cavity structure with IC layers and the top dielectric and bottom oxidized DBRs. The oxidized DBR effectively blocks light emission practically for all tilted angles, redirects it into the top DBR and, as a result, reduces the bottom leakage to 3%. Together with the positive effect from top dielectric DBR, it leads to an increase in photon-extraction efficiency up to 42% for an NA of 0.7.

Further enhancement of the photon-extraction efficiency can be obtained by including radial Bragg gratings and 2 μm-diameter oxide-confined aperture also in the hybrid device design. The impact of the radial 2nd-order trench pattern formed in the top DBR on the light extraction efficiency for the circular half-pillar based on the hybrid 2λ-cavity structure is shown in Figure 5. As it follows from our simulations the ring trench patterning results in a noticeable enhancement in the extraction efficiency in this case due to reduction of the sidewall leakage. Together with the insertion of the 40nm-thick oxide-confined aperture at antinode, it leads to the reduction of the sidewall leakage to 33% (maintaining the bottom leakage around 3%) and, as a result, an increase in extraction efficiency of emission from the hybrid 2λ-cavity up to 51% within NA=0.7. Interestingly, moving the oxide-confined aperture at the local intensity minimum (not shown) leads to a more pronounced in-plane leakage (~38%) and degradation of the extraction efficiency (NA=0.7) back to 46%.

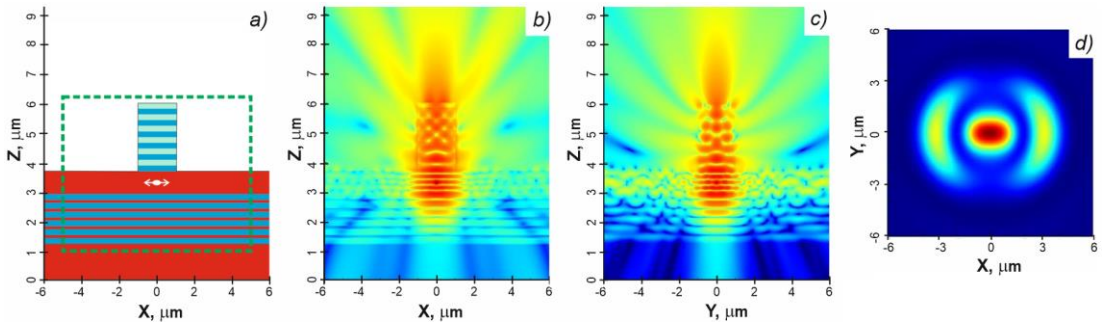

Figure 4. 1.3 μm range circular half-pillar based on hybrid 2λ-cavity structure with IC layers and dielectric and oxidized DBRs: refractive index profile in X-Z plane (a) and on-resonance electric field intensity distribution in X-Z (b), Y-Z (c), X-Y (d) planes for the fundamental mode HE_{11}.

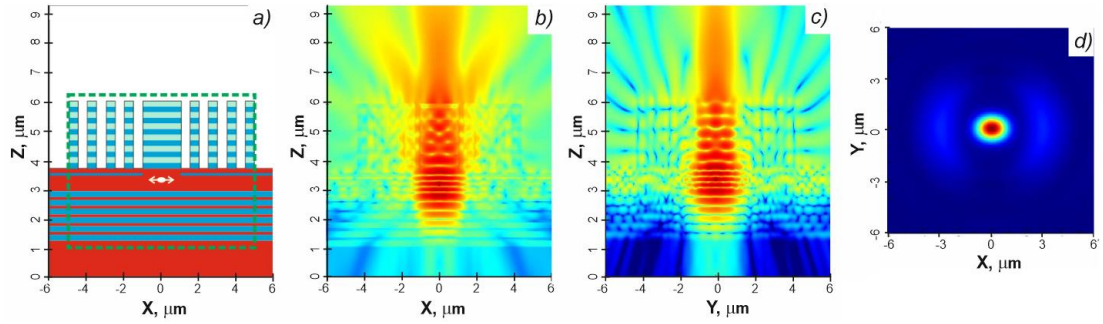

Figure 5. 1.3 μm range circular radial DBR microcavity half-pillar based on hybrid 2λ-cavity structure with IC layers, dielectric and oxidized DBRs and oxide-confined aperture: refractive index profile in X-Z plane (a) and on-resonance electric field intensity distribution in X-Z (b), Y-Z (c), X-Y (d) planes for the fundamental mode HE_{11}.

Note that the significant part of the sidewall leakage in the investigated microcavities is associated with the light emitted in-plane. Figure 6 shows the results of a 1D calculation of the optical modes in different planar microcavities. A standard vertical microcavity always has a few waveguide modes depending on cavity design. For example, the fundamental and second-order waveguide modes exist in the hybrid 2λ-cavity structure with IC layers and dielectric and oxidized DBRs. To solve this problem of multi-mode operation the so-called passive cavity concept was proposed [14]. Recently, the brightness of the micro-LED emitting in the orange spectral range at ~610 nm was enhanced up to ~95% with a narrow far-field pattern [15]. In our case the dielectric passive cavity is inserted below the top dielectric DBR and separated from the semiconductor cavity with IC-layers and the active region by 1-period thick intermediate dielectric DBR (the hybrid passive cavity structure). The semiconductor cavity is thinned down to approximately λ/4 to increase the anti-waveguiding effect, while the thick matching $AlGa_xO_y$ and SiO_2 layers were inserted to maximize interaction of the QD e with the vertical optical mode of the proposed microcavity structure. As it follows from Figure 6.b, the modes of the planar waveguide except one tilted mode are suppressed. In the frame of the simple analysis of the planar structure, this mode cannot be suppressed. Possibly the insertion of the oxide–confined aperture near the active region and the ring trench pattern formed in dielectric part can further prohibit the in-plane light propagation and redirect all emitted light in the vertical direction.

Figure 7 shows simulation results for circular half-pillar based on the hybrid passive cavity structure with IC layers and the top dielectric and bottom oxidized DBRs. As expected, the field intensity is mainly concentrated in the dielectric part, while the light propagation in the direction towards the substrate is almost suppressed (the bottom leakage ~2%). However, the propagation of the emitted light in the lateral plane is not fully prohibited. In addition the significant part of emission still passes through the micro-pillar side, which gives the sidewall leakage of 36%. Nevertheless the photon-extraction

efficiency of the circular half-pillar based on the hybrid passive cavity structure can be increased from 42% up to 58% (NA=0.7) as compared to the circular half-pillar based on the hybrid 2λ-cavity structure.

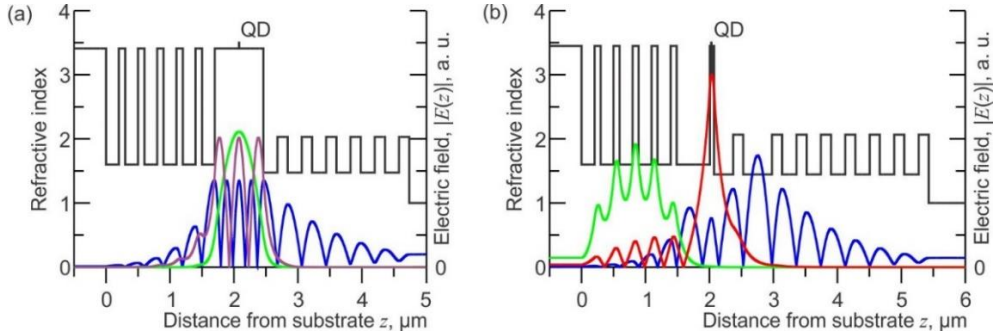

Figure 6. Calculated refractive index (black curves) and electric field strength profiles of different modes for hybrid 2λ-cavity structure (a) and hybrid passive cavity structure (b) with IC layers and dielectric and oxidized DBRs. Blue curves: vertical modes, green and purple curves: waveguide modes, red curve: high–order waveguide (tilted) mode.

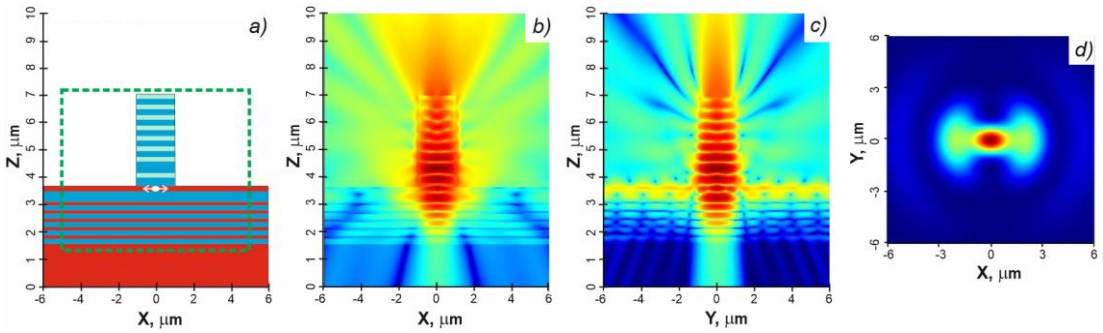

Figure 7. 1.3 μm range circular half-pillar based on hybrid passive cavity structure with IC layers and dielectric and oxidized DBRs: refractive index profile in X-Z plane (a) and on-resonance electric field intensity distribution in X-Z (b), Y-Z (c), X-Y (d) planes for the fundamental mode HE_{11}.

As it follows from Figure 8, the etching of the 2nd-order ring trench pattern through the dielectric part enables one to block a portion of light propagated in the lateral direction and travelling from the pillar side. Furthermore, the oxide-confined aperture partially suppresses the in-plane propagation of the light in the anti-waveguiding cavity. As a result, the bottom leakage is almost prohibited to 1%, while the side emission in the radial microcavity half-pillar is reduced to 16%. Due to such remarkable change in the field distribution the photon-extraction efficiency rises up to 75% (NA=0.7), which includes also a small fraction of the side emission directed towards the collection optics with the mentioned NA. Note that employing the passive cavity concept also allow one to shrink the near-field emission pattern, so nearly Gaussian transverse mode profile, which improves the coupling efficiency into a single-mode fiber can be improved by optimizing the radial Bragg gratings in the future.

In summary, we have carried out 3D FDTD simulations of light extraction efficiency from different types of micro-cavity structures which can potentially be used for the realization of ultra-bright electrically driven QD-based SPSs in the telecom O-band at 1.3 μm. The broad stop-band bottom DBRs blocks the light propagation practically at all tilted angles and suppresses the emission leakage below the active cavity. The radial trench pattern formed in the top DBR can potentially redirect upwards some part of the side emission. The passive cavity concept allows almost complete suppression of the sidewall emission and provides overall photon extraction efficiency up to 83% and extraction efficiency of ~75% within numerical aperture 0.7. This approach allows one to etch the passive cavity region through without risking of nonradiative recombination of carriers on the etched sidewalls and thus enables exploiting the full strength of the Purcell effect.

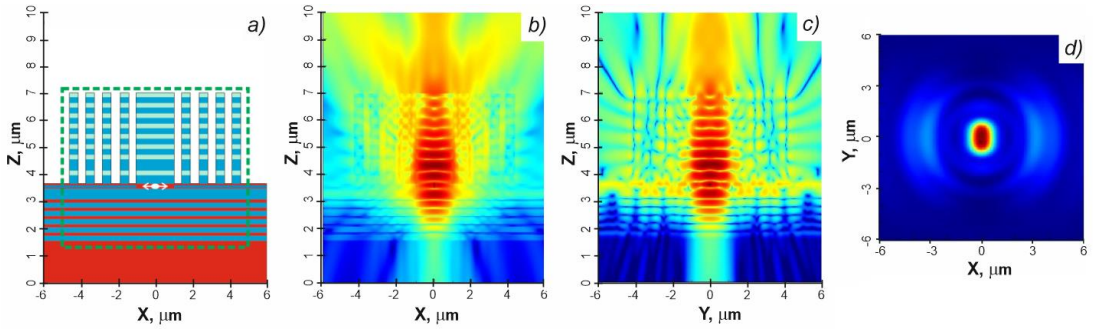

Figure 8. 1.3 μm range circular radial DBR microcavity half-pillar based on hybrid passive cavity structure with IC layers, dielectric and oxidized DBRs and oxide-confined aperture: refractive index profile in X-Z plane (a) and on-resonance electric field intensity distribution in X-Z (b), Y-Z (c), X-Y (d) planes for the fundamental mode HE_{11}.

Acknowledgments
The reported study was funded by the Joint Research Project of the Russian Foundation for Basic Research (RFBR) № 20-52-12006 and Deutsche Forschungsgemeinschaft (DFG) Re2974/24-1.

References
[1] Michler P *Quantum Dots for Quantum Information Technologies*, Springer 2017
[2] Schlehahn A et al. 2015 *Applied Physics Letters* **107** 041105
[3] Claudon J et al. 2010 *Nature Photonics* **4** 174
[4] Unsleber S et al. 2016 *Optics Express* **24** 8539
[5] Schlehahn A et al. 2016 *APL Photonics* **1** 011301
[6] Liu J et al. 2019 *Nature nanotechnology* **14** 586
[7] Chen Z–S et al. 2017 *Nanoscale Research Letters* **12** 378
[8] Srocka N et al. 2018 *AIP Advances* **8** 085205
[9] Kim J –H et al. 2016 *Optica* **3** 577
[10] Rickert L et al. 2019 *Optics Express* **27** 36824
[11] Schneider P-I et al. 2018 *Optics Express* **26** 8479
[12] Ho Y L D et al. 2007 *IEEE Journal of Quantum Electronics* **43** 462
[13] Asplund C et al. 2001 *Journal of Applied Physics* **90** 794
[14] Shchukin V et al. 2016 *Proceedings of SPIE* **9766** 976609
[15] Ledentsov N Jr et al. 2017 *Proceedings of SPIE* **10124** 101240O